

## INTERACTION OF BUBBLES RISING IN A VISCOELASTIC LIQUID WITH NEGATIVE WAKES

Hafiz Usman Naseer<sup>1</sup>  
Koc University  
Istanbul, Turkey

Zaheer Ahmed<sup>2</sup>  
MUET, SZAB Campus  
Khairpur, Pakistan

Metin Muradoglu<sup>3</sup>  
Koc University  
Istanbul, Turkey

### ABSTRACT

*The present study aims to investigate the interactions of buoyancy-driven bubbles rising in an otherwise quiescent viscoelastic liquid with negative wakes. The FENE-P model is used to model fluid rheology of the viscoelastic medium. Interface-resolved three-dimensional simulations are first performed to examine the formation of a negative wake behind a single buoyant bubble in a viscoelastic ambient liquid. Simulations are then performed to investigate complex interactions of three-dimensional bubbles with negative wakes for a range of governing non-dimensional parameters.*

### INTRODUCTION

Gas-liquid multiphase flows exist in a wide range of natural processes and technological applications. Therefore, it has been an active area of research to understand the dynamics of these multiphase flows. The interface-resolved numerical simulations of multiphase flows have been proved to be a difficult task mainly due to the existence of a sharp interface between liquid and gaseous phases that continuously evolve in time and space and may even undergo topological changes such as breakup and coalescence. The material properties such as viscosity and density vary discontinuously across the interfaces, which adds a further complexity to the problem. The situation exacerbates even further when one or both phases are viscoelastic. Viscoelastic liquids are common in biological flows mainly due to existence of biological polymers such as proteins and in many engineering applications such as polymer melts. The viscoelastic fluids exhibit many exotic behaviors that have been widely utilized to achieve useful functions in a myriad technological application. In particular, a negative wake is formed behind a buoyancy-driven rising bubble in viscoelastic liquid under certain conditions [Joseph, et al., 1995]. The formation of negative wake behind a single bubble has been studied experimentally [Pilz, et al., 2007] and computationally [Niethammer, et al., 2019] but the

---

<sup>1</sup> GRA, Department of Mechanical Engg, Koc University, Istanbul, Turkey. Email: hnaseer19@ku.edu.tr

<sup>2</sup> Lecturer, Department of Mechanical Engg, Mehran University, Pakistan. Email: zaheerahmed@muethkp.edu.pk

<sup>3</sup> Professor, Department of Mechanical Engg, Koc University, Istanbul, Turkey. Email: mmuradoglu@ku.edu.tr

interactions of bubbles with negative wakes is yet to be fully explored. The present study aims to computationally investigate the complex flow caused by strong interactions of bubbles with negative wakes. Viscoelastic fluids are usually modeled as a fluid filled with elastic bead and spring dumbbells representing long-chain polymers. Several such models have been developed and successfully used to simulate the behavior of viscoelastic fluids in a wide range of flow conditions. In particular, FENE-P [Bird, et al., 1980] and EPTT [Phan-Thien, et al., 1977] models have proved to be able to capture some of the most important features of viscoelastic fluids such as turbulent drag reduction by polymer additives and shear thinning and have been widely used in direct numerical simulation (DNS) of viscoelastic turbulent flows. They are also used in the present study.

Several attempts have been made in the recent decades to capture the dynamics of a gas bubble rising in a viscoelastic liquid under buoyancy. If the bubble size increases beyond a critical volume, a negative wake is produced behind the trailing edge of the bubble, which is responsible for producing "velocity jump" in the terminal velocity of this rising bubble. Pitz and Brenn [Pilz, et al., 2007] performed detailed experiments and reported a jump discontinuity of rise velocity as the bubble volume exceeded a critical limit. They also found a universal correlation of non-dimensional numbers at which this velocity discontinuity occurs. Niethammer et al. [Niethammer, et al., 2019] performed numerical simulations using a volume-of-fluid (VOF) and successfully reproduced the experimental results. They used the EPTT model to model the rheology of viscoelastic medium. Velocity jump is clearly seen as the bubble volume exceeded the critical limit. This velocity jump occurs primarily due to negative wake behind the trailing edge of the bubble where the flow velocity reverses its direction with respect to the bubble rise velocity. This formation of negative wake is a continuous dynamic process which changes the stress distribution around the bubble, thus producing a jump in the rise velocity. Cao and Macián-Juan [Cao, et al., 2020] investigated the dynamics and deformation of three-dimensional bubble rising in a viscoelastic liquid under different combination of non-dimensional numbers. They employed the Oldroyd-B model for the fluid rheology and demonstrated that strain in the fluid is associated with the shear induced by the rising bubble. D. Fraggedakis, 2016 [Fraggedakis, et al., 2016] examined the abrupt increase in the rise velocity of an isolated bubble rising in a viscoelastic medium. They predicted shapes of the larger bubbles when both inertia and elasticity are present. Tagawa et al. [Tagawa, et al., 2014] studied the effect of surfactants on path instability of a rising bubble. Mohammad Vahabi, 2021 [Vahabi, et al., 2021] demonstrated the behavior of two inline bubbles ascending in an Oldroyd-B viscoelastic model. Bunner and Tryggvason [Bunner, et al., 2003] predicted bubble deformation due to change in the properties of bubble flows. Zenit and Magnaudet [Zenit, et al., 2008] discussed a shape-controlled process in detail for path instability of rising spheroidal air bubbles. Legendre et al. [Legendre, et al., 2012] provided an excellent insight into the deformation of gas bubbles in liquids. Lu et al. [Lu, et al., 2017] studied the effects of insoluble surfactant on turbulent bubbly flows in vertical channels which are a common flow type in industrial applications. Lu and Tryggvason [Lu, et al., 2008] examined the effect of bubble deformability in a vertical channel for an upflow. Young et al. [Young, et al., 1959] studied the motion of bubbles in a vertical temperature gradient. Tripathi et al. [Tripathi, et al., 2015] shed some light on the dependence of surface tension on temperature. Balla et al. [Balla, et al., 2019] studied three dimensional effects of non-isothermal bubble rise dynamics in a self-wetting fluid. Yuan et al. [Yuan, et al., 2021] studied the peculiar behaviours at critical volumes of a three-dimensional bubble with special emphasis on comparing different viscoelastic models. Although the phenomenon is yet to be fully understood, Kemiha et al. [Kemiha, et al., 2006] discussed the origin of negative wake behind a bubble rising in non-Newtonian fluids. You et al. [You, et al., 2008] presented a finite volume formulation for simulating drop motion in a viscoelastic two-phase system. Several other attempts have also been made to understand the dynamics and the role of elasticity at different combinations of non-dimensional numbers.

The importance and applications of rising bubbles in viscoelastic mediums can be found abundantly in literature. Rodríguez-Rodríguez et al. [Rodríguez-Rodríguez, et al., 2015] has

presented a summary of microbubbles generation and their applications in industry and medicines.

We examine the complex interactions of buoyant bubbles rising in different orientations under the conditions where the negative wake occurs behind the bubbles. The FENE-P model is used to model the liquid viscoelasticity. Extensive simulations are performed for a wide range of governing parameters using a fully three dimensional and parallelized front-tracking method [Unverdi, et al., 1992, Muradoglu, et al., 2008, Muradoglu, et al., 2014, Ahmed, et al., 2020].

### COMPUTATIONAL SETUP AND NUMERICAL METHOD

Following the work of Izbassarov and Muradoglu [Izbassarov, et al., 2015], the effects of surface tension can be included as a force in momentum equation. Thus, the Navier-Stokes equations for the entire domain can be written in the following form:

$$\frac{\partial \rho \mathbf{u}}{\partial t} + \nabla \cdot (\rho \mathbf{u} \mathbf{u}) = -\nabla p + \nabla \cdot \mu (\nabla \mathbf{u} + \nabla \mathbf{u}^T) + \nabla \cdot \boldsymbol{\tau} + \mathbf{g} \Delta \rho + \int [\sigma \kappa \mathbf{n}] \delta(\mathbf{x} - \mathbf{x}_f) dA \quad (1)$$

where  $\mathbf{u}$  is the velocity vector,  $p$  is the pressure field,  $\boldsymbol{\tau}$  is the extra stress tensor due to the polymers,  $\rho$  and  $\mu$  are the discontinuous density and viscosity fields, respectively. The last term in Eq. (1) represents the body force due to surface tension where  $\sigma$  is the surface tension coefficient,  $\kappa$  is twice the mean curvature, and  $\mathbf{n}$  is a unit vector normal to the bubble interface.

The momentum equation is supplemented by the incompressibility condition:

$$\nabla \cdot \mathbf{u} = 0 \quad (2)$$

It is assumed that material properties remain constant while following the fluid particle, i.e.,

$$\frac{D\rho}{Dt} = 0 \quad (3)$$

$$\frac{D\mu}{Dt} = 0 \quad (4)$$

The density and viscosity vary discontinuously across the fluid interface and are given by:

$$\rho = \rho_0 I(\mathbf{x}, t) + \rho_i (1 - I(\mathbf{x}, t)) \quad (5)$$

$$\mu = \mu_0 I(\mathbf{x}, t) + \mu_i (1 - I(\mathbf{x}, t)) \quad (6)$$

where the subscript  $i$  and  $o$  represent the bubble and the bulk fluids respectively.  $I$  is an indicator function which is unity in the bulk fluid and zero in the bubble.

The FENE-P model is used to account for the extra stresses due to the polymers in the viscoelastic liquid. This model belongs to the family of the finitely extensible nonlinear elastic (FENE) models and can be written as

$$\frac{\partial \mathbf{B}}{\partial t} + \nabla \cdot (\mathbf{u} \mathbf{B}) - (\nabla \mathbf{u})^T \cdot \mathbf{B} - \mathbf{B} \cdot \nabla \mathbf{u} = -\frac{1}{\lambda} (\mathbf{F} \mathbf{B} - \mathbf{A} \mathbf{I}) \quad (7)$$

$$\mathbf{F} = \frac{L^2}{L^2 - \text{trace}(\mathbf{B})}; \quad \mathbf{A} = \frac{L^2}{L^2 - 3}$$

where  $\mathbf{B}$  is the conformation tensor,  $\lambda$  is the polymer relaxation time and  $\mathbf{I}$  is the identity tensor. After computing the conformation tensor, the polymeric stress tensor is computed as

$$\boldsymbol{\tau} = \frac{\mu_p}{\lambda} (\mathbf{F} \mathbf{B} - \mathbf{A} \mathbf{I}) \quad (8)$$

where  $\mu_p$  is the polymeric viscosity. The flow equations (1) and (2) are solved using the front-tracking method [Izbassarov, et al., 2015]. The momentum and the continuity equations are solved on a stationary staggered (Eulerian grid) and are discretized by second-order central difference approximations for the spatial derivatives except for the convective terms for which a QUICK scheme is used in the momentum equation and a fifth order WENO-Z scheme is

used in the viscoelastic model. The time integration is achieved by a second order predictor-corrector method [Muradoglu, et al., 2014].

A rectangular domain is selected for all the cases in the present study. Length of the domain in streamwise direction ( $y$  direction) is chosen as  $40R$ , whereas this length is  $8R$  in the other two dimensions. Periodic boundary conditions are selected in the  $y$  and  $x$  directions whereas no slip condition is imposed in the wall normal direction ( $z$  direction). For all the cases of single bubble, initial location of the bubble is  $0.4R$  in the  $x, y$  and  $z$  directions (Fig 1).

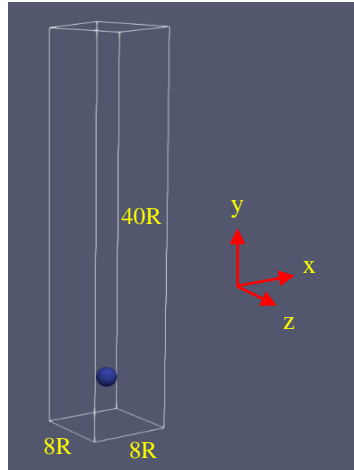


Figure 1: Rectangular computational domain with bubble at its initial location.

## RESULTS AND DISCUSSION

First, the code is validated by matching the results with an already published case in the literature. For this purpose, a rectangular domain is selected to duplicate the results of Yuan et al. (2020) for the Weissenberg number  $Wi = UR/\lambda = 10$  and  $Eo = g\Delta\rho R^2/\sigma = 100$ , where  $R$  is the radius of the undeformed spherical bubble which is used as the length scale and  $U = \sqrt{gR}$  as the velocity scale. Bubble rise velocity and time are normalized using the velocity scale  $U$  and time scale  $T = U/R$ , respectively. The rise velocity of bubble is plotted in Fig. 2 as a function of time together with the computational result of Yuan et al. (2020). As seen, the present results are in good agreement with the results of Yuan et al. (2020) demonstrating the accuracy of the present results.

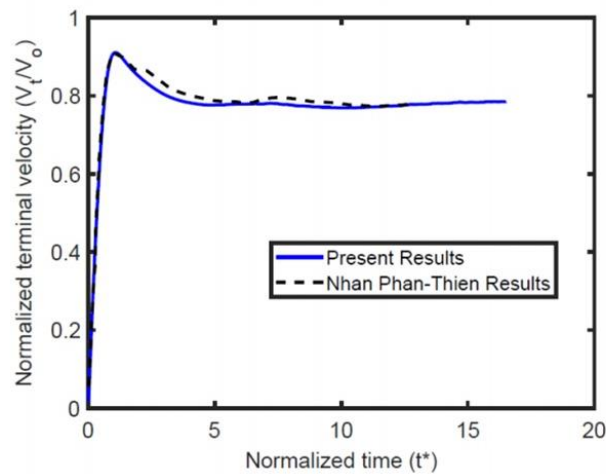


Figure 2: Time evolution of the bubble rise velocity of a single bubble in an otherwise quiescent viscoelastic liquid.

## INTERACTIONS OF BUBBLES

In order to observe the interaction between negative wakes, two bubbles of equal sizes ( $R=0.1$ ) were placed in parallel to each other with a distance of  $0.5R$  in between their centers. Non-dimensional numbers were kept the same ( $Wi = 10, Eo = 100, Ga = 3.91$ ) as in the case of the single bubble so that both bubbles could produce negative wakes. As shown in Fig. 3, the two bubbles started to rise due to buoyancy force and their mutual distance started to increase. The bubble shapes are significantly different than the single bubble case and the negative wake takes more time to appear as the 'eye dropped' shape on the trailing edge kept on changing its orientation with the bubble rise. Finally, when the mutual distance between the two bubbles became  $4R$ , the orientation of negative wake becomes perpendicularly downward and the two bubbles start to rise independent of each other with their terminal velocity. However, their terminal velocity is significantly different than that of the single bubble case.

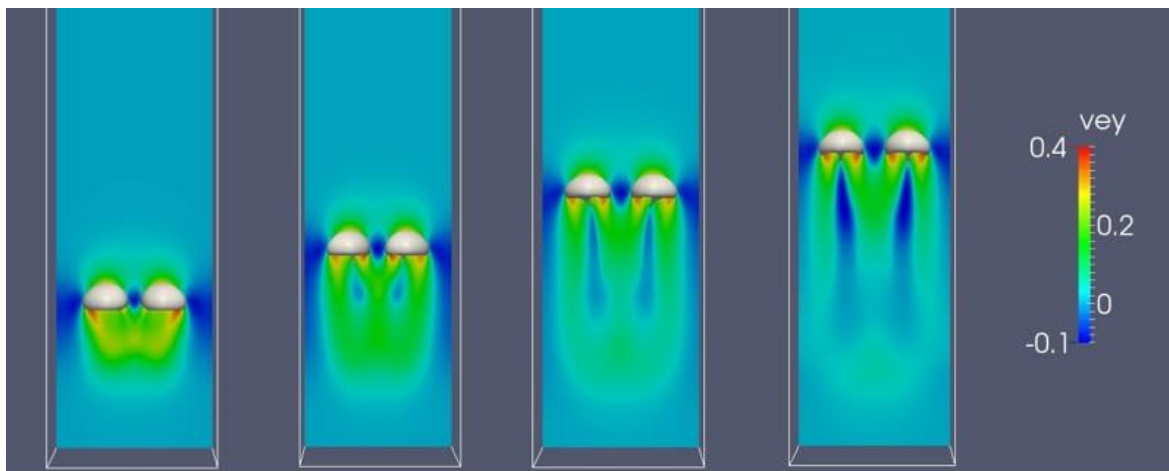


Figure 3: Time evolution of velocity contours between two bubbles started with horizontal initial alignment.

In the next case, two bubbles of equal sizes were placed in-line to each other with a mutual distance of  $4R$  between their centers. As the two bubbles start to rise in the viscoelastic medium under the buoyancy force, their mutual distance starts to decrease as shown in Figs. 4 and 5. The cusped shape of the upper bubble is found to be significantly different than that of the lower bubble. The rise velocity of upper bubble is the same as that in case of single bubble whereas the lower bubble rises faster, decreasing the mutual distance and ultimately merges with the upper bubble. An interesting observation is the absence of negative wake for the upper bubble as can be seen in Fig. 4, whereas the lower bubble produces a relatively smaller negative wake before it merges with the upper bubble.

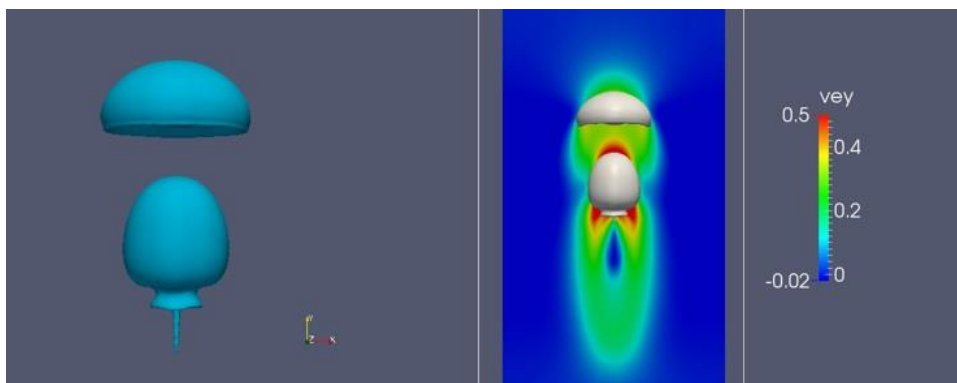


Figure 4: Shape of in-line bubbles of equal size at  $t=0.08$ .

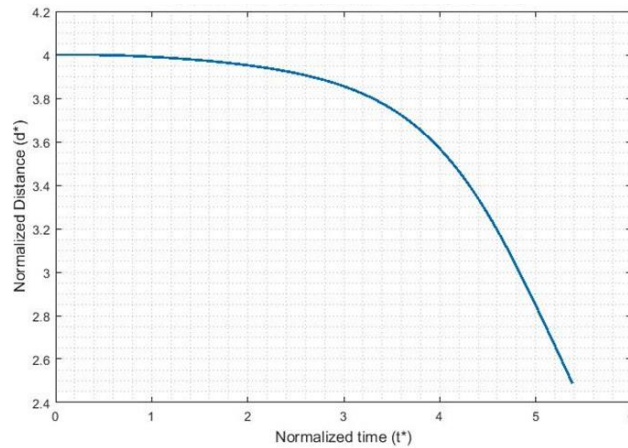


Figure 5: Time evolution of the distance between bubbles when they are initialized in line vertically.

To determine the interaction distance, simulations are performed for the various values of the initial distance between the in-line bubbles. Under the stated non-dimensional numbers and a bubble radius of  $R = 0.1$ , the distance for which the bubbles cease to interact is found to be  $16R$ .

The strong interaction between the bubbles is subsided as the Eötvös number ( $Eo$ ) is reduced. Eötvös number measures the importance of gravitational force as compared to surface tension force. Therefore, bubble interaction in the buoyancy driven flow is strongly affected by Eötvös number. When Eötvös number is reduced from 100 to 1, the interaction between bubbles becomes almost negligible. The bubbles rise almost independently producing their respective negative wakes (Fig 6b). The cusp shape of each bubble in this case is similar to that of a single bubble case but the strength of negative wake is slightly decreased. The phenomenon is attributed to slightly lower viscoelastic stress concentration around the lower hemisphere of each bubble (Fig 6c) which results in lower terminal velocity as compared to single bubble case. The difference is found to be almost 9.36% (Fig 7). Note that Fig. 6a shows the initial orientation and mutual distance between the bubbles.

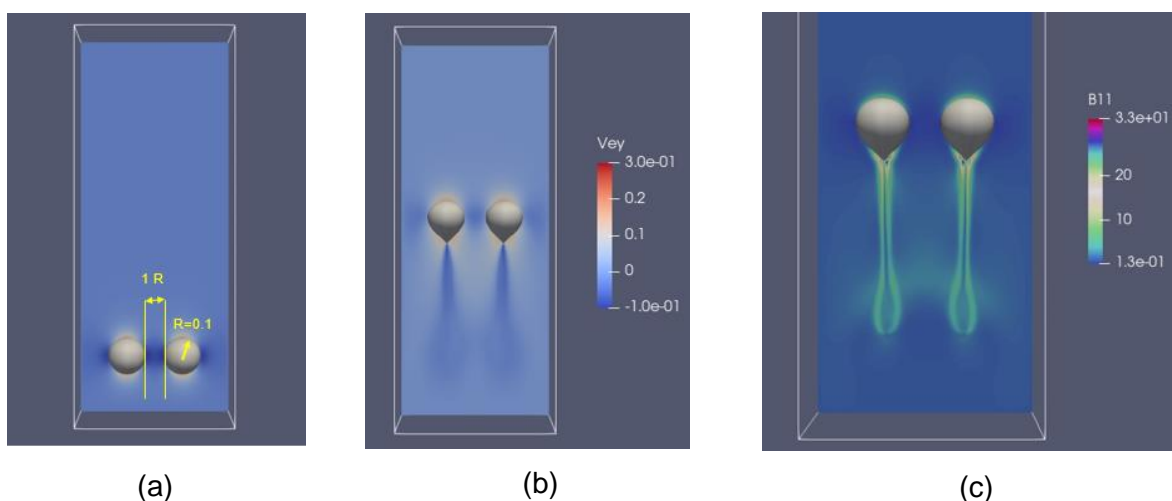


Figure 6: Time evolution of velocity contours between two bubbles at low Eötvös number ( $Eo=1$ ) at (a)  $t=0$  (b)  $t=5$  (c)  $t=7$ .

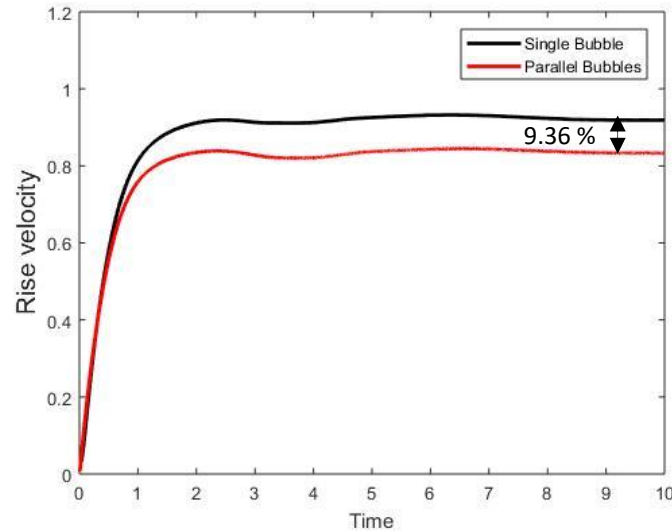


Figure 7: Comparison of bubble rise velocities between single and two parallel bubbles with an initial distance of  $1R$

The terminal velocity of a buoyancy driven bubble in viscoelastic medium is a strong function of its shape as well. The widely studied phenomenon of velocity jump beyond a critical bubble volume primarily depends upon its cusped shape. Although this phenomenon is not fully explained yet, it is the shape of the bubble which ultimately gives rise to a negative wake behind its trailing edge. This bubble shape is mainly dependent upon dynamic stress distribution around its upper and lower hemispheres as it rises in a viscoelastic medium. In order to observe the effect of polymeric viscosity on bubble shapes, the non-dimensional parameter  $\beta = \mu_s / (\mu_s + \mu_p)$  is increased gradually. This parameter represents the ratio between solvent viscosity to total viscosity of the fluid. As the value of  $\beta$  increases, polymeric viscosity ( $\mu_p$ ) decreases and the shape of the bubbles change from ‘tear drop’ to a more spherical lower hemisphere (Fig 8). This change in bubble shape reduces the strength of negative wake behind its trailing edge and ultimately the bubble rise velocity is reduced (Fig 9). With lower rise velocities, bubbles travel comparatively less distance in the streamwise direction with higher value of  $\beta$ .

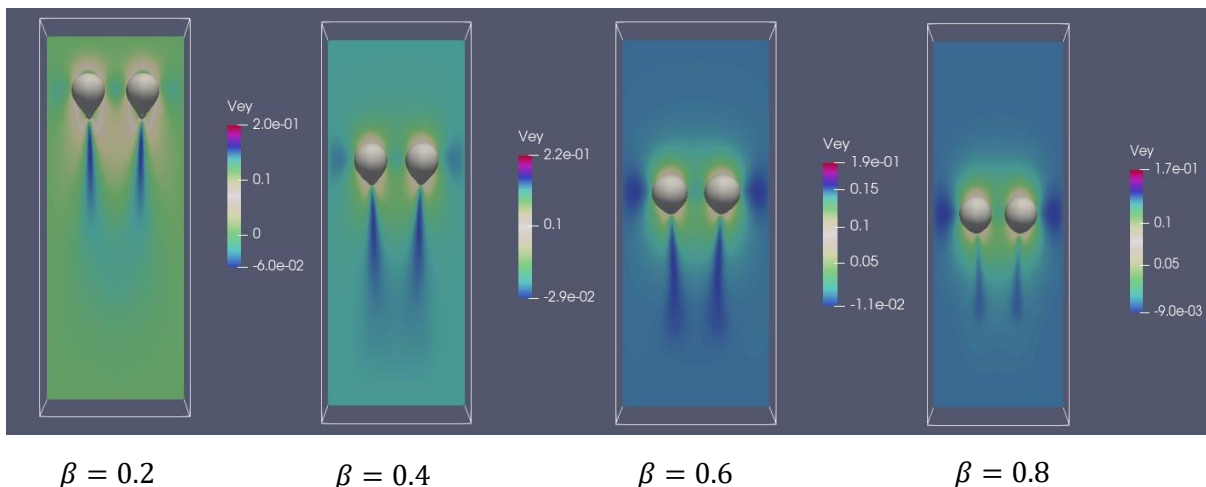


Figure 8: Effect of  $\beta$  on bubble shapes and associated negative wakes at  $t = 10$ . All four cases were initialized with a mutual distance of  $1R$  at  $t = 0$  with  $Eo = 1$ .

As the value of  $\beta$  increases beyond a certain limit, the polymeric effects become so negligible that the rise velocity matches with that of the corresponding Newtonian case with no negative wake.

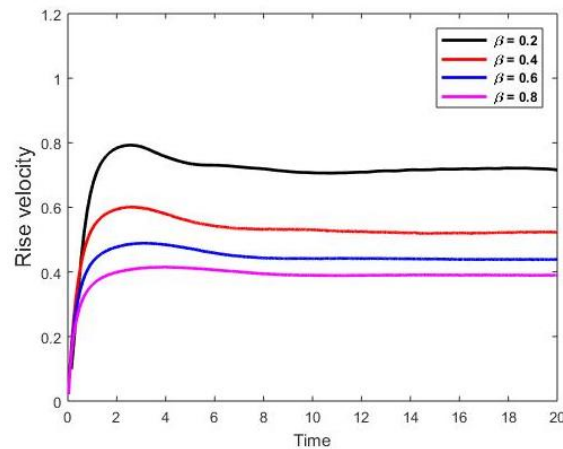


Figure 9: Effect of  $\beta$  on bubble rise velocity for  $Eo=1$ .

## CONCLUSION

Multiple cases of parallel and in-line bubbles with a combination of equal and variable sizes are simulated to observe the production and interactions of negative wakes produced by the bubbles rising in an otherwise quiescent viscoelastic liquid. The bubble rise velocity is found to be a strong function of the bubble sizes, wall effects and the initial distance between bubble centers.

The interaction between bubbles is subsided as the Eötvös number is reduced. As this number represents the relative measure between gravitational and surface tension forces, buoyancy driven flows are strongly impacted by even minute change in this number. As the Eötvös number is reduced, the change in surface tension directly affects the shape of the bubble. The change in cusped shape of the bubble is mainly attributed to change in viscoelastic stress distribution around its upper and lower hemispheres. As a result, not only the interaction with the nearby bubble is completely changed but also the strength of negative wake is impacted. It is observed that the overall bubble rise velocity is decreased by decreasing the Eötvös number.

The widely studied phenomenon of velocity discontinuity is observed in non-Newtonian fluids only. Bubble shape, negative wake behind its trailing edge and velocity jump are the main attributes of this dynamic process which is yet to be fully understood. It is observed that by increasing the viscosity ratio ( $\beta$ ), bubble shape is transformed from 'eye drop' to a more spherical shape with a significant reduction in its rise velocity. At a very high value of  $\beta$ , terminal velocity of the bubble almost matches with that of a Newtonian fluid.

## ACKNOWLEDGEMENTS

We acknowledge financial support from the Scientific and Technical Research Council of Turkey (TUBITAK) grant No.115M688 in the initial stage of this work and Turkish Academy of Sciences (TUBA).



## REFERENCES

- Ahmed Z. [et al.]** Turbulent bubbly channel flows: Effects of soluble surfactant and viscoelasticity [Journal] // *Computers and Fluids*. - 2020. - Vol. 212. - p. 104717.
- Ahmed Z., Izbassarov D. and Muradoglu M.** Effects of soluble surfactant on lateral migration of a bubble in a pressure driven channel flow [Journal] // *International Journal of Multiphase Flow*. - 2020. - Vol. 126. - p. 103251.
- Balla M. [et al.]** Non-isothermal bubble rise dynamics in a self-rewetting fluid: three-dimensional effects [Journal] // *Journal of Fluid Mechanics*. - 2019. - Vol. 858. - pp. 689-713.
- Bird R.B., Dotson P.J. and Johnson N.L.** Polymer solution rheology based on a finitely extensible bead-spring chain model [Journal] // *J. Non-Newtonian Fluid Mech.* - 1980. - 2-3 : Vol. 7. - pp. 213-235.
- Bunner B. and Tryggvason G.** Effect of bubble deformation on the properties of bubbly flows [Journal] // *J. Fluid Mech.* - 2003. - Vol. 495. - pp. 77-118.
- Cao Y. and Macián-Juan R.** Numerical study of the central breakup behaviors of a large bubble rising in quiescent liquid [Journal] // *Chemical Engineering Science*. - 2020. - Vol. 225. - p. 115804.
- Clift R., Grace, J. R., & Weber, M. E.** Bubbles, drops, and particles. [Book]. - 2005.
- Farooqi M.N., Izbassarov D. and Muradoglu M.** Communication analysis and optimization of 3D front tracking method for multiphase flow simulations [Journal] // *The International Journal of High Performance Computing Applications*. - 2019. - 1 : Vol. 33. - pp. 67-80.
- Farooqi M.N., Muradoglu M. and Unat D.** Communication analysis and optimization of 3D front tracking method for multiphase flow simulations [Journal]. - [s.l.] : *The International Journal of High Performance Computing Applications*, 2019. - 1 : Vol. 33. - pp. 67-80.
- Fraggedakis D., Pavlidis M. and Tsamopoulos J.** On the velocity discontinuity at a critical volume of a bubble rising in a viscoelastic fluid [Journal] // *J. Fluid Mech.* - 2016. - Vol. 789. - pp. 310-346.
- Izbassarov D. and Muradoglu M.** A front-tracking method for computational modeling of viscoelastic two-phase systems [Journal] // *The Journal of Non-Newtonian Fluid Mechanics*. - 2015. - Vol. 223. - pp. 122-140.
- Joseph D. D. and Feng J.** The negative wake in a second-order fluid [Journal] // *Journal of Non-Newtonian Fluid Mechanics*. - 1995. - 2-3 : Vol. 57. - pp. 313-320.
- Kemiha M. [et al.]** Origin of the negative wake behind a bubble rising in non-Newtonian fluids [Journal] // *Chemical Engineering Science*. - 2006. - 12 : Vol. 61. - pp. 4041-4047.
- Kupferman Raanan Fattal and Raz** Constitutive laws for the matrix-logarithm of the conformation tensor [Journal] // *Journal of Non-Newtonian Fluid Mechanics*. - 10 November 2004.
- Legendre D., Zenit R. and Velez-Cordero J.R.** On the deformation of gas bubbles in liquids [Journal] // *Physics of Fluids*. - 2012. - Vol. 24. - p. 043303.
- Lu J. and Muradoglu M., Tryggvason, G.** Effect of insoluble surfactant on turbulent bubbly flows in vertical channels [Journal] // *International Journal of Multiphase Flow*. - 2017. - Vol. 95. - pp. 135-143.
- Lu J. and Tryggvason G.** Effect of bubble deformability in turbulent bubbly upflow in a vertical channel [Journal] // *Physics of Fluids*. - 2008. - 4 : Vol. 20. - p. 040701.
- Lu J., Muradoglu M. and Tryggvason G.** Effect of insoluble surfactant on turbulent bubbly flows in vertical channels [Journal] // *International Journal of Multiphase Flow*. - 2017. - Vol. 5. - pp. 135-143.
- M.van Sint Annal N.G.Deen and J.A.M.Kuipers** Numerical simulation of gas bubbles behaviour using a three-dimensional volume of fluid method [Journal] // *Chemical Engineering Science*. - June 2005. - pp. Pages 2999-3011.

- Metin Muradoglu Gretar Tryggvason** A front-tracking method for computation of interfacial flows with soluble surfactants [Journal] // Journal of Computational Physics. - 2008. - pp. 2238–2262.
- Metin Muradoglu Gretar Tryggvason** Simulations of soluble surfactants in 3D multiphase flow [Journal] // Journal of Computational Physics. - 2014.
- Mitsuhiro Ohtaa Kei Onoderaa, Yutaka Yoshidaa, and Mark Sussmanb** Three-Dimensional Numerical Simulations of a Rising Bubble in a Viscoelastic FENE-CR Model Fluid [Conference] // AIP Conference Proceedings 1027, 896. - 2008.
- Muradoglu M. and Tryggvason G.** A front-tracking method for computation of interfacial flows with soluble surfactants [Journal] // Journal of Computational Physics. - 2008. - 4 : Vol. 227. - pp. 2238-2262.
- Muradoglu M. and Tryggvason G.** Simulations of soluble surfactants in 3D multiphase flow [Journal] // Journal of Computational Physics. - 2014. - Vol. 274. - pp. 737-757.
- Muradoglu M. and Tryggvason G.** Simulations of soluble surfactants in 3D multiphase flow [Journal] // Journal of Computational Physics. - 2014. - Vol. 274. - pp. 737-757.
- Niethammer M. [et al.]** An extended volume of fluid method and its application to single bubbles rising in a viscoelastic liquid [Journal] // Journal of Computational Physics. - 2019. - Vol. 387. - pp. 326-355.
- Phan-Thien N. and Tanner R.I.** A new constitutive equation derived from network theory [Journal] // Journal of Non-Newtonian Fluid Mechanics. - 1977. - 4 : Vol. 2. - pp. 353-365.
- Pilz C. and Brenn G.** On the critical bubble volume at the rise velocity jump [Journal] // J. Non-Newtonian Fluid Mech.. - 2007. - 2-3 : Vol. 145. - pp. 24-138.
- Renardy M.** Mathematical analysis of viscoelastic flows. [Journal] // Society for Industrial and Applied Mathematics.. - (2000).
- Rodríguez-Rodríguez J. [et al.]** Generation of Microbubbles with Applications to Industry and Medicine [Journal] // Annual Review of Fluid Mechanics. - 2015. - Vol. 47. - pp. 405-429.
- Tagawa Y., Takagi S. and Matsumoto Y.** Surfactant effect on path instability of a rising bubble [Journal] // J. Fluid Mech.. - 2014. - Vol. 738. - pp. 124-142.
- Tripathi M.K. [et al.]** Non-isothermal bubble rise: non-monotonic dependence of surface tension on temperature [Journal] // J. Fluid Mech.. - 2015. - Vol. 763 . - pp. 82-108.
- Unverdi S.O. and Tryggvason G.** [Journal] // Journal of Computational Physics. - 1992. - 1 : Vol. 100. - pp. 25-37.
- Vahabi M., Hadavandmirzaei H. and Safari H.** Interaction of a pair of in-line bubbles ascending in an Oldroyd-B liquid: A numerical study [Journal] // European Journal of Mechanics / B Fluids. - 2021. - Vol. 85. - pp. 413-429.
- Wenjun Yuan Nhan Phan-Thien** Dynamics and deformation of a three-dimensional bubble rising in viscoelastic fluids [Journal] // Journal of Non-Newtonian Fluid Mechanics. - 2020.
- You R., Borhan A. and Haj-Hariri H.** A finite volume formulation for simulating drop motion in a viscoelastic two-phase system [Journal] // Journal of Non-Newtonian Fluid Mechanics. - 2008. - 2-3 : Vol. 153. - pp. 109-129.
- Young N.O., Goldstein J.S. and Block M.J.** The motion of bubbles in a vertical temperature gradient [Journal] // Journal of Fluid Mechanics. - 1959. - 3 : Vol. 6 . - pp. 350-356.
- Yuan W. [et al.]** On peculiar behaviours at critical volumes of a three-dimensional bubble [Journal] // Journal of Non-Newtonian Fluid Mechanics. - 2021. - Vol. 293. - p. 104568.
- Zaheer Ahmed Daulet Izbassarov, Metin Muradoglu, Outi Tammissola,** Turbulent bubbly channel flows: Effects of soluble surfactant and viscoelasticity [Journal] // Computers and Fluids. - 2020.
- Zenit R. and Magnaudet J.** Path instability of rising spheroidal air bubbles: A shape-controlled process [Journal] // Physics of Fluids. - 2008. - Vol. 20 . - p. 061702.